



Through-Thickness Residual Stress Evaluations for Several Industrial Thermal Spray Coatings Using a Modified Layer-Removal Method

D.J. Greving, E.F. Rybicki, and J.R. Shadley

Residual stresses are inherent in thermal spray coatings because the application process involves large temperature gradients in materials with different mechanical properties. In many cases, failure analysis of thermal spray coatings has indicated that residual stresses contribute to reduced service life. An established method for experimentally evaluating residual stresses involves monitoring deformations in a part as layers of material are removed. Although the method offers several advantages, applications are limited to a single isotropic material and do not include coated materials. This paper describes a modified layer-removal method for evaluating through-thickness residual stress distributions in coated materials. The modification is validated by comparisons with three-dimensional finite-element analysis results. The modified layer-removal method was applied to determine through-thickness residual stress distributions for six industrial thermal spray coatings: stainless steel, aluminum, Ni-5Al, two tungsten carbides, and a ceramic thermal barrier coating. The modified method requires only ordinary resistance strain-gage measuring equipment and can be relatively insensitive to uncertainties in the mechanical properties of the coating material.

1. Introduction

THERMAL spray coatings are widely used in industrial applications that require surface and thermal property improvements such as corrosion and wear resistance (Ref 1) and thermal barrier properties (Ref 2). Residual stresses are created by the thermal spray coating application process, which involves large temperature changes and materials that often have different mechanical and thermal properties. Tensile residual stresses have been found to contribute to failures in many different material joining processes, including welding and weld repairs (Ref 3). In thermal spray coatings, residual stresses frequently have been identified or suspected as a contributing factor to shortened service life (Ref 2, 4-7). Failure modes in thermal spray coatings that are attributable, at least in part, to residual stresses include spalling, cracking, and debonding.

Experimental evaluation of residual stresses in thermal spray coatings enables relation of the total state of stress in the coating to observed failures, prediction of service life, development of residual stress improvement strategies, and development of quality assurance procedures for coating processes. Determination of residual stresses in materials can be done using both destructive and nondestructive methods. X-ray diffraction (Ref 8) is a frequently used nondestructive method, usually provides information at points very near the surface and requires accurate knowledge of the mechanical properties of the material being evaluated. With destructive methods, deformations are moni-

tored as strains relax when parts of a structure are machined away. The hole-drilling method (Ref 9) is a semidestructive method that has been used to estimate residual stresses in thermal spray coatings. This method evaluates residual stresses at points near the surface and also depends on accurate knowledge of the mechanical properties of the material. Like the conventional layer-removal method, the hole-drilling procedure was developed for a single isotropic material and does not account for different mechanical properties of a substrate and coating, or for coating thickness.

The modified layer-removal method (Ref 10) is a destructive technique that has been used to determine through-thickness residual stress distributions in thermal spray coatings. An extension of the conventional layer-removal method (Ref 11, 12), this technique factors in coating thickness and the different mechanical properties of the substrate and the coating.

2. Modified Layer-Removal Method

2.1 Definitions

The layer-removal method is based on the concept that removing a layer from the surface of a plate or beam with residual stresses releases a force and moment acting on the remaining piece. It is presumed that the remaining piece is large enough and the layer removed small enough so that the change in strain through the thickness of the remaining piece is linear. A strain rosette (gage) on the remaining piece records the change in strain on the surface opposite the face where the layer was removed. The stresses in the layer removed and the change in stresses of the remaining piece can be calculated from force and moment equilibrium, the linear strain change assumption, the

Keywords finite-element analysis, layer removal, mechanical properties, strain-gage method

D.J. Greving, E.F. Rybicki, and J.R. Shadley, Mechanical Engineering Department, The University of Tulsa, Tulsa, OK 74104-3189, USA.

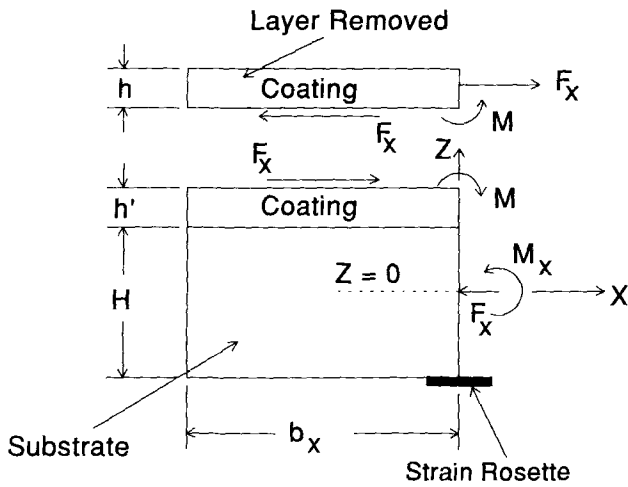


Fig. 1 Free-body diagram for layer-removal method applied to a thermal spray coated specimen

strain rosette readings, and the stress-strain properties of the material.

One key assumption of the conventional layer-removal method (Ref 11) is that the Young's modulus and Poisson's ratio are the same throughout the specimen. For thermal spray coatings, however, the mechanical properties of the substrate and the coating are not necessarily equal, and it is possible for the coating Young's modulus to be only a small fraction of the substrate modulus. In order to account for this difference in material properties, a modification to the layer-removal method was developed. Consider the layer-removal free-body diagram shown in Fig. 1. The force acting on the layer in the X-direction is denoted by F_x . The force and moment acting on the remaining piece are related to F_x by force and moment equilibrium conditions. The thickness of the substrate is H , the thickness of the layer removed is h , and the remaining coating thickness is h' . The length of the piece in the X-direction is b_x . Not shown in Fig. 1 is b_y , the length of the piece in the Y-direction. The Young's modulus and Poisson's ratio of the substrate (base) for directions in the plane of the coating are E_b and ν_b , respectively. The corresponding properties of the coating are E_c and ν_c . The remainder of the derivation follows the mechanics of composite materials analysis for bending and stretching a two-material nonsymmetric plate (Ref 13).

Because some confusion may exist about the sign of the stress in the layer removed and its relation to the sign of the strain rosette data, it is helpful to consider the analysis for the step of putting the layer back on the remaining piece. Then the change in strain of interest is for "replacing" the layer and is equal to the negative of the change in strain rosette data obtained for removing the layer.

2.2 Relation between Layer Stresses and Strain Changes in the Substrate

For convenience, the reference plane ($Z=0$) has been located at the center of this thickness of the remaining piece. The change in strain distribution through this thickness, due to replacing the layer on the remaining piece, is a linear function of z :

$$\begin{aligned}\epsilon_x &= \epsilon_{x0} + K_x Z \\ \epsilon_y &= \epsilon_{y0} + K_y Z\end{aligned}\quad (\text{Eq 1})$$

In Eq 1, ϵ_x and ϵ_y are the linear strain distributions through the thickness of the remaining piece, ϵ_{x0} and ϵ_{y0} are the middle plane strains, and K_x and K_y are the middle plane curvatures for the X-direction and the Y-direction, respectively. The stress-strain equations for isotropic plane stress behavior for the substrate and the coating have the form:

$$\begin{Bmatrix} \sigma_x \\ \sigma_y \end{Bmatrix} = E' \begin{bmatrix} 1 & \nu \\ \nu & 1 \end{bmatrix} \begin{Bmatrix} \epsilon_x \\ \epsilon_y \end{Bmatrix}\quad (\text{Eq 2})$$

where σ_x and σ_y are the stresses in the X-direction and the Y-direction respectively; ν is either ν_b , the Poisson's ratio for the substrate, or ν_c , the Poisson's ratio for the coating; and E' is either $E'_b = E_b/(1 - \nu_b^2)$ for the substrate or $E'_c = E_c/(1 - \nu_c^2)$ for the coating.

2.3 Resultant Forces and Moments

It is convenient to work with resultant forces and resultant moments (Ref 13), which are defined as the force per unit length, F'_x and F'_y , and the moment per unit length, M'_x and M'_y . In terms of the forces and dimensions shown in Fig. 1,

$$\begin{aligned}F'_x &= \frac{F_x}{b_x} \\ F'_y &= \frac{F_y}{b_y} \\ M'_x &= \frac{M_x}{b_x} \\ M'_y &= \frac{M_y}{b_y}\end{aligned}\quad (\text{Eq 3})$$

Resultant forces and resultant moments are denoted by primes and are related to stresses by:

$$\begin{aligned}\begin{Bmatrix} F'_x \\ F'_y \end{Bmatrix} &= \int_{-(H+h')/2}^{(H+h')/2} \begin{Bmatrix} \sigma_x \\ \sigma_y \end{Bmatrix} dz \\ \begin{Bmatrix} M'_x \\ M'_y \end{Bmatrix} &= \int_{-(H+h')/2}^{(H+h')/2} \begin{Bmatrix} \sigma_x \\ \sigma_y \end{Bmatrix} z dz\end{aligned}\quad (\text{Eq 4})$$

Substituting Eq 1 and 2 into Eq 4 gives

$$\begin{Bmatrix} F'_x \\ F'_y \\ M'_x \\ M'_y \end{Bmatrix} = \begin{bmatrix} A_{11} & A_{12} & B_{11} & B_{12} \\ A_{12} & A_{22} & B_{12} & B_{22} \\ B_{11} & B_{12} & D_{11} & D_{12} \\ B_{12} & B_{22} & D_{12} & D_{22} \end{bmatrix} \begin{Bmatrix} \epsilon_{x0} \\ \epsilon_{y0} \\ K_x \\ K_y \end{Bmatrix}\quad (\text{Eq 5})$$

where

$$A_{11} = A_{22} = E'_b H + E'_c h' \quad (\text{Eq 6})$$

$$A_{12} = \nu_b E'_b H + \nu_c E'_c h' \quad (\text{Eq 7})$$

$$B_{11} = B_{22} = (E'_c - E'_b) H h' / 2 \quad (\text{Eq 8})$$

$$B_{12} = (\nu_c E'_c - \nu_b E'_b) H h' / 2 \quad (\text{Eq 9})$$

$$D_{11} = D_{22} = \frac{E'_b}{12} H(H^2 + 3h'^2) + \frac{E'_c}{12} h'(h'^2 + 3H^2) \quad (\text{Eq 10})$$

$$D_{12} = \frac{\nu_b E'_b}{12} H(H^2 + 3h'^2) + \frac{\nu_c E'_c}{12} h'(h'^2 + 3H^2) \quad (\text{Eq 11})$$

2.4 Equations for Modified Layer-Removal Method

Changes in strains at the gaged surface, $\Delta\epsilon_{xG}$ and $\Delta\epsilon_{yG}$, that occur when the layer is replaced can be related to strains ϵ_{x0} and ϵ_{y0} at the midplane using Eq 1:

$$\begin{aligned} \epsilon_{x0} &= \Delta\epsilon_{xG} + K_x(H + h')/2 \\ \epsilon_{y0} &= \Delta\epsilon_{yG} + K_y(H + h')/2 \end{aligned} \quad (\text{Eq 12})$$

where, because of the "replacement of the layer" concept adopted for the analysis, $\Delta\epsilon_{xG}$ and $\Delta\epsilon_{yG}$ are the changes in strains due to replacing the layer on the remaining piece (the negative of the strain change due to removing the layer). Substituting Eq 12 into Eq 5 gives

$$\begin{aligned} \begin{Bmatrix} F'_x \\ F'_y \\ M'_x \\ M'_y \end{Bmatrix} &= \begin{bmatrix} A_{11} & A_{12} & B_{11} & B_{12} \\ A_{12} & A_{22} & B_{12} & B_{22} \\ B_{11} & B_{12} & D_{11} & D_{12} \\ B_{12} & B_{22} & D_{12} & D_{22} \end{bmatrix} \begin{Bmatrix} \Delta\epsilon_{xG} \\ \Delta\epsilon_{yG} \\ 0 \\ 0 \end{Bmatrix} \\ &+ \begin{Bmatrix} K_x(H + h')/2 \\ K_y(H + h')/2 \\ K_x \\ K_y \end{Bmatrix} \end{aligned} \quad (\text{Eq 13})$$

The resultant forces and resultant moments acting on the remaining piece are related to the stress in the removed layer, shown in Fig. 1, by:

$$\begin{Bmatrix} F'_x \\ F'_y \\ M'_x \\ M'_y \end{Bmatrix} = - \begin{Bmatrix} \sigma_{xL} h \\ \sigma_{yL} h \\ h\sigma_{xL}(H + h' + h)/2 \\ h\sigma_{yL}(H + h' + h)/2 \end{Bmatrix} \quad (\text{Eq 14})$$

where σ_{xL} and σ_{yL} are stresses in the layer removed. Equations 13 and 14 give four equations in terms of the four unknowns σ_{xL} , σ_{yL} , K_x , and K_y :

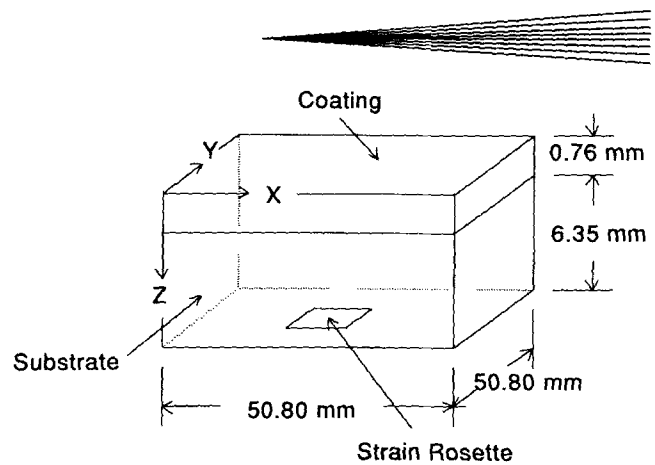


Fig. 2 Thermal spray coated specimen for finite-element model

$$\begin{bmatrix} h & 0 & A_{11}T + B_{11} & A_{12}T + B_{12} \\ 0 & h & A_{12}T + B_{12} & A_{22}T + B_{22} \\ Th & 0 & B_{11}T + D_{11} & B_{12}T + D_{12} \\ 0 & Th & B_{12}T + D_{12} & B_{22}T + D_{22} \end{bmatrix} \begin{Bmatrix} \sigma_{xL} \\ \sigma_{yL} \\ K_x \\ K_y \end{Bmatrix} = - \begin{bmatrix} A_{11} & A_{12} \\ A_{12} & A_{22} \\ B_{11} & B_{12} \\ B_{12} & B_{22} \end{bmatrix} \begin{Bmatrix} \Delta\epsilon_{xG} \\ \Delta\epsilon_{yG} \end{Bmatrix} \quad (\text{Eq 15})$$

where

$$T = (H + h')/2 \text{ and } T' = (H + h' + h)/2 \quad (\text{Eq 16})$$

Solving Eq 15 gives the stresses in the layer removed (σ_{xL} and σ_{yL}) and the changes of curvature in the remaining piece (K_x and K_y). From this information, the change in stress distribution in the remaining piece can be evaluated using Eq 1, 2, and 12.

3. Validation of the Modified Layer-Removal Method

Before the modified layer-removal method was used to evaluate residual stresses in thermal spray coatings, it was validated for selected reference cases with established solutions. The reference solutions were based on results from finite-element models of thermal spray coatings on a substrate. The finite-element model contained residual stresses in the coating and substrate generated by applying a temperature change in the coating. Five cases were considered. In each case, a layer was removed from the coating. The residual stresses in the removed layer were obtained from the finite-element solution and served as the reference solution. Changes in strains on the substrate, where a strain rosette (gage) would be located, were also obtained from results of the finite-element model. These strain changes were treated as strain gage readings, as though actual laboratory strain measurements had been made, and were used as input data to the modified layer-removal method. The stresses in the removed layer were then calculated by the modified layer-removal method. The calculated stresses were compared to the reference solution from the finite-element analysis to evaluate

the accuracy of the modified method. Two cases will be discussed here. Case 1 consists of a thermal spray coating on a steel substrate, and case 2 involves a coating on an aluminum substrate. Specimen dimensions for each case are shown in Fig. 2. The substrate is 6.35 mm (0.250 in.) thick, and the coating is 0.762 mm (0.030 in.) thick. The lateral dimensions of the specimen are 50.80 by 50.80 mm (2.00 by 2.00 in.). In each case, a 0.127 mm (0.005 in.) thick layer of coating was removed and the change in strains at the gage location, on the back surface of the specimen shown in Fig. 2, was evaluated from the finite-element results.

The mechanical properties of the coating and substrate and the thickness dimensions needed for the modified layer-removal method are listed in Table 1. Representative modulus and Poisson's ratio values were selected for the steel and aluminum substrates. It is recognized that the modulus and Poisson's ratio of coating materials are not always available. For purposes of validation of the modified layer-removal method, the mechanical property values shown in Table 1 were selected.

A change of temperature in the coating was specified to generate a residual stress state in the finite-element model of the coated substrate. This temperature change was selected to illustrate the predictive capability of the modified layer-removal method rather than to accurately portray residual stresses in a thermal spray coating. The residual stresses in the layer were ob-

tained from the finite-element model and compared to the values calculated using the modified layer-removal method. The comparison is presented in Table 2.

Table 2 shows that the modified layer-removal method calculates the residual stresses in the layer to within 0.4% of the finite-element solution. This provides confidence in the capability of the modified method for thermal spray coatings. If the conventional layer-removal method (Ref 11) were used for cases 1 and 2, the calculated residual stresses in the layer would be in error in the range of 30 to 40% (Table 2).

Table 3 shows the sensitivity of the modified layer-removal method to uncertainties in the mechanical properties of the coating. Residual stress values from the modified method are compared to values obtained from the three-dimensional finite-element model using case 1 inputs from Table 1. Then it was assumed that the values of the coating modulus, E_c , and the coating Poisson's ratio, ν_c , were estimated to be 20% higher than the actual values, and residual stresses were calculated by the modified method. Using the exact values of the mechanical properties, the modified layer-removal method has a 0.1% difference when compared to the three-dimensional finite-element results. For the same case, but where the coating modulus used has an uncertainty of 20%, the layer stress computed by the modified method had a difference of only 0.4% when compared to the finite-element model results. This difference obtained for an uncertain Poisson's ratio was 0.1%. This shows that a relatively large uncertainty in coating properties (20%) can have only a small influence on the residual stresses determined by the modified layer-removal method.

Table 1 Input values for modified layer-removal method

Property	Case 1	Case 2
E_b	207.0 GPa	68.9 GPa
ν_b	0.3	0.2
E_c	14.0 GPa	14.0 GPa
ν_c	0.25	0.25
H	6.35 mm	6.35 mm
h	0.127 mm	0.127 mm
h'	0.635 mm	0.635 mm
$\Delta\epsilon_{xG}$	1.924×10^{-5}	3.047×10^{-5}
$\Delta\epsilon_{yG}$	1.924×10^{-5}	3.047×10^{-5}

4. Parting-Out and Splitting Steps

Residual stress evaluations by the modified layer-removal method can also be applied to geometries that are more complicated than test coupons. The specimen may have been parted out from a larger piece. In this technique, surface strain changes are recorded while a coupon of the desired dimensions is cut from

Table 2 Comparison of coating residual stresses from layer-removal methods and finite-element model

Case	Modified layer-removal method		Finite-element model		Difference, %	Conventional layer-removal method		Finite-element model		Difference, %
	σ_{xL} , MPa	σ_{yL} , MPa	σ_{xL} , MPa	σ_{yL} , MPa		σ_{xL} , MPa	σ_{yL} , MPa	σ_{xL} , MPa	σ_{yL} , MPa	
1	109.8	109.8	109.9	109.9	0.1	152.2	152.2	109.9	109.9	38.5
2	53.9	53.9	54.2	54.2	0.4	70.3	70.3	54.2	54.2	29.8

Table 3 Sensitivity of modified layer-removal method to mechanical property uncertainty

Conditions	E_b , MPa	ν_b	E_c , MPa	ν_c	Residual stress, MPa	Difference, %
3-D finite-element model reference	207.0	0.30	14.0	0.25	109.9	...
Modified ν_c layer-removal method						
Exact E_c and ν_c	207.0	0.30	14.0	0.25	109.8	0.1
20% uncertainty in E_c	207.0	0.30	16.8	0.25	110.4	0.4
20% uncertainty in ν_c	207.0	0.30	14.0	0.30	110.0	0.1

the more complex part. Then the stress state that existed in the coupon before separation is computed from the measured surface strain changes and suitable assumptions about the behavior of the coupon as it is cut from the parent part (Ref 14). In some instances, the substrate of a thermal spray coated specimen may be too thick to obtain sizable strain changes as layers are removed from the coating. For such cases, a splitting step is used to reduce the thickness of the substrate before applying the layer-removal procedure. Changes in stress due to splitting (and parting-out, if applicable) are added to the stresses obtained by layer removal.

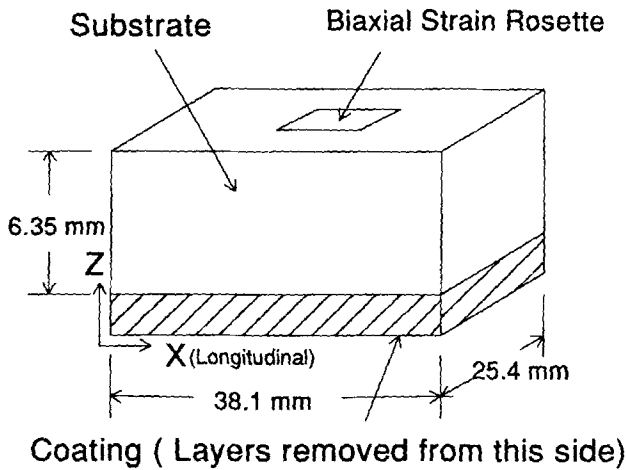


Fig. 3 Residual stress specimens ready for layer removal

5. Application to Industrial Thermal Spray Coatings

Figure 3 shows the dimensions of a typical residual stress specimen. Figures 4 to 10 show through-thickness residual stress distributions for the stress in the X-direction for seven different coatings. Layers from the coating side were removed by wet polishing. Readings were taken from the biaxial strain rosette mounted on the substrate surface. The modified layer-removal method was applied to calculate the residual stresses. Each figure shows the results for one to four duplicate specimens of each coating type. The horizontal axis shows distance, Z, through the thickness of the specimen as measured from the surface of the coating. The vertical axis shows the residual stress, σ_x , in the X-direction (longitudinal) of the specimens.

Figure 4 shows the through-thickness residual stress distribution for a Wall Colmonoy (Wall Colmonoy Corp., Madison Heights, MI) aluminum coating applied with a Colmonoy Model WG-500 (Wall Colmonoy Corp., Madison Heights, MI) wirespray gun. The AISI 1018 steel substrate was stress relieved in accordance with ASM recommendations (Ref 15). Specimens were grit blasted and cleaned prior to coating. No preheat was applied. The final coating thickness was approximately 0.762 mm (0.030 in.). A substrate modulus of 200.0 GPa (29.0×10^6 psi) and a substrate Poisson's ratio of 0.3 were used for the residual stress analysis. A coating modulus of 68.9 GPa (10.0×10^6 psi) and a coating Poisson's ratio of 0.3 were used for calculating the residual stresses. Coating properties were assumed to be those of wrought aluminum, as better estimates were not available.

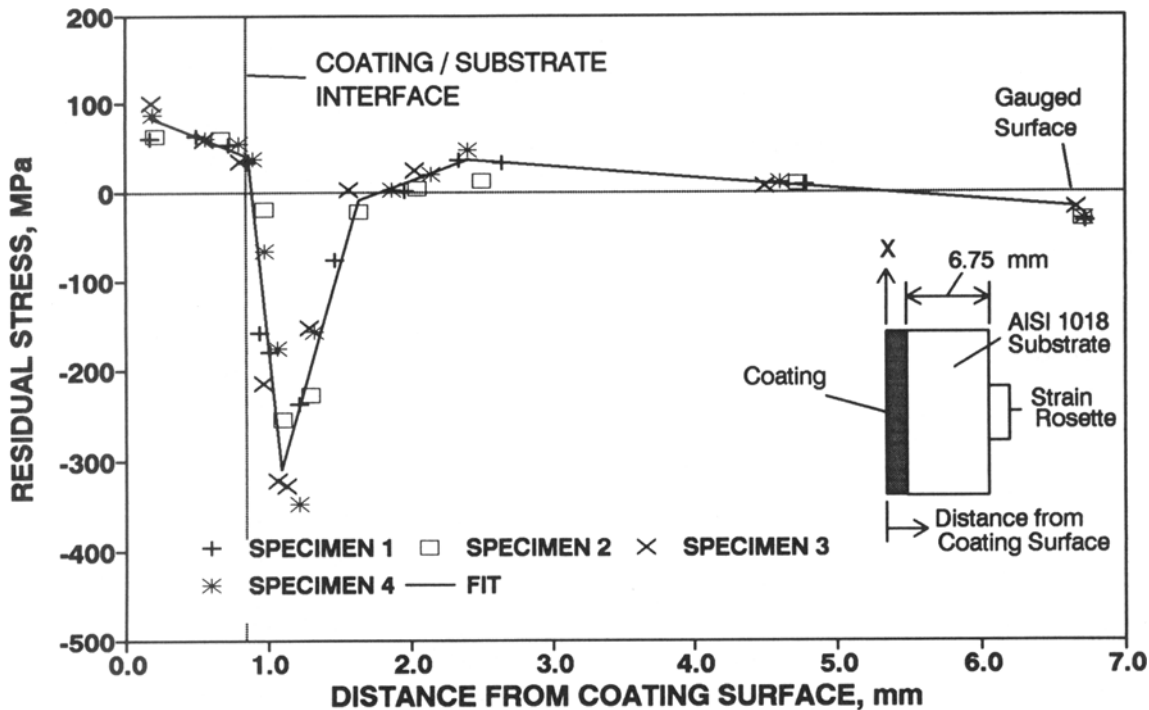


Fig. 4 Residual stress distribution for aluminum coating on an AISI 1018 steel substrate

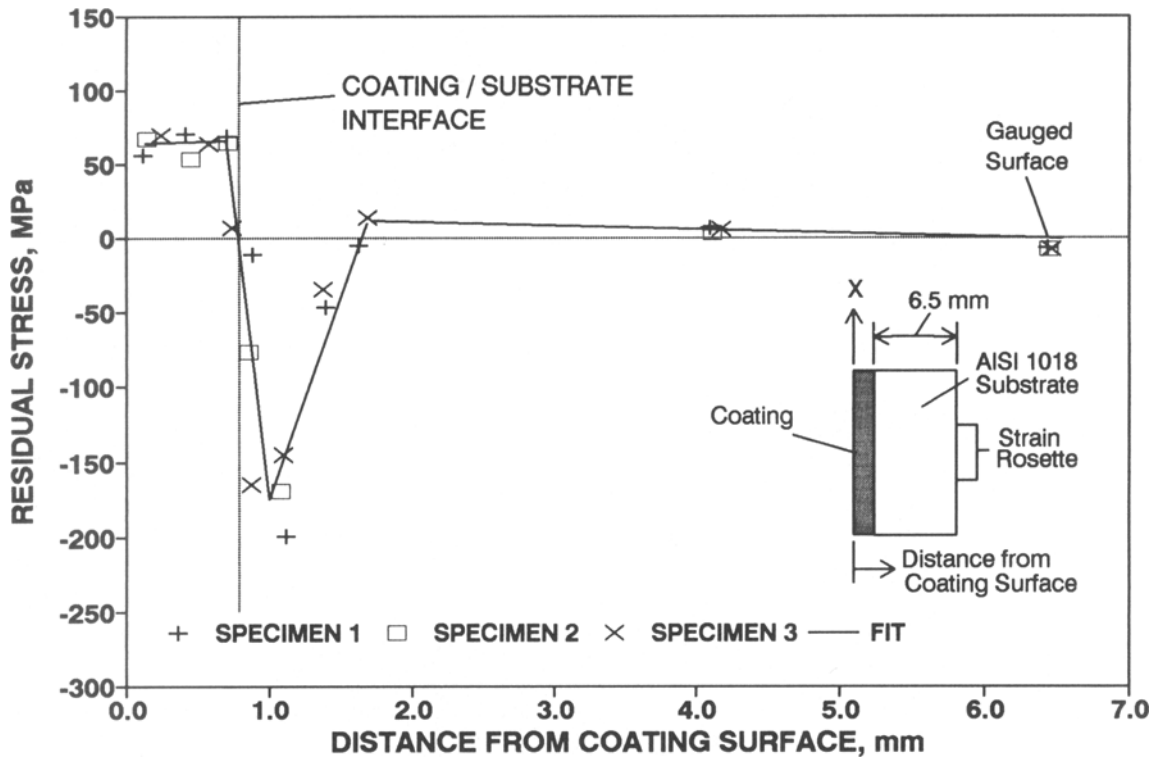


Fig. 5 Residual stress distribution for stainless steel coating on an AISI 1018 steel substrate

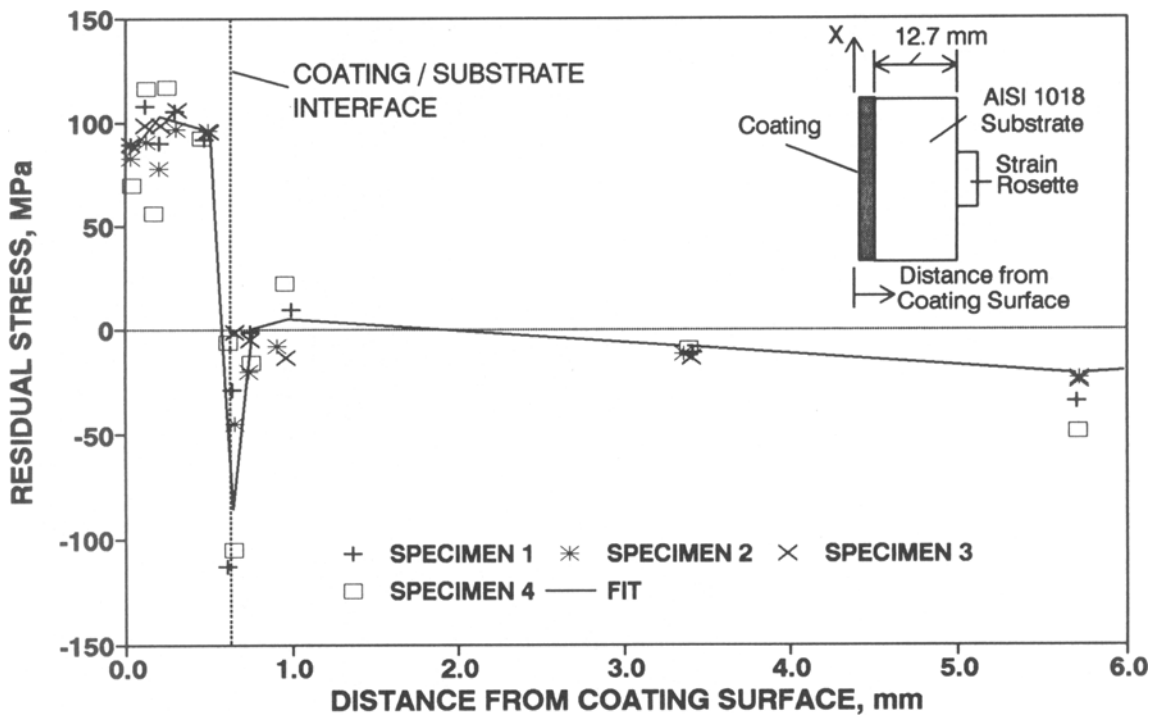


Fig. 6 Residual stress distribution for Ni-5Al coating on an AISI 1018 steel substrate

Figure 5 shows the through-thickness residual stress distribution for a Walcoloy #5 (Wall Colmonoy Corp., Madison Heights, MI) austenitic stainless steel coating applied with a

Colmonoy Model WG-500 (Wall Colmonoy Corp., Madison Heights, MI) wirespray gun. The AISI 1018 steel substrate was stress relieved. Specimens were grit blasted and cleaned prior to

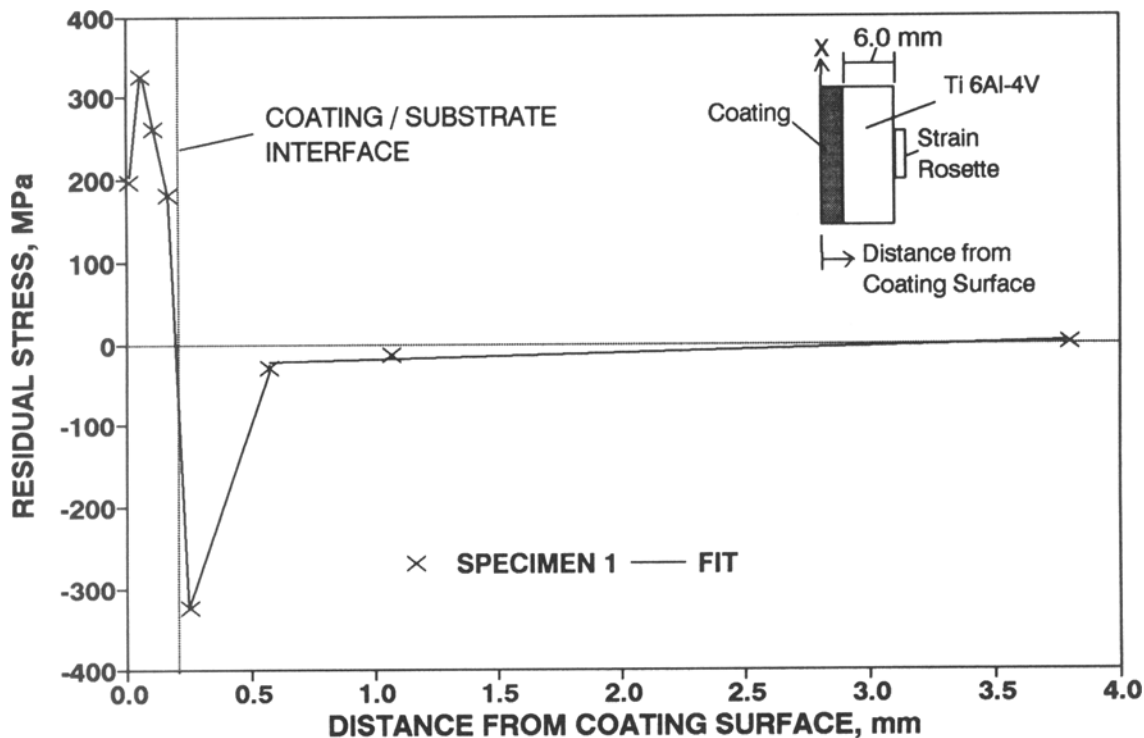


Fig. 7 Residual stress distribution for WC-Co coating applied by HVOF-A on a titanium substrate

coating. No preheat was applied. The final coating thickness was approximately 0.762 mm (0.030 in.). A substrate modulus of 200.0 GPa (29.0×10^6 psi) and a substrate Poisson's ratio of 0.3 were used for the residual stress analysis. A coating modulus of 58.6 GPa (8.5×10^6 psi) and a coating Poisson's ratio of 0.3 were used for calculating the residual stresses. The coating modulus was found by conducting a cantilevered beam test on a coated specimen.

Figure 6 shows the through-thickness residual stress distribution for a Ni-5Al Tafa Bondarc 75B (Hobart Tafa Technologies, Inc., Concord, NH) coating applied with a Hobart Tafa Model 9000 (Hobart Tafa Technologies, Inc., Concord, NH) wirespray system. The AISI 1018 steel substrate was stress relieved. Specimens were grit blasted and cleaned prior to coating. No preheat was applied. The final coating thickness was approximately 0.762 mm (0.030 in.). A substrate modulus of 200.0 GPa (29.0×10^6 psi) and a substrate Poisson's ratio of 0.3 were used for the residual stress analysis. A coating modulus of 68.9 GPa (10.0×10^6 psi) and a coating Poisson's ratio of 0.3 were used for calculating the residual stresses. The coating modulus was found by conducting a cantilevered beam test on a coated specimen.

Figures 4 to 6 indicate a tensile stress through the thickness of the coating. These results also show that a compressive stress zone exists in the substrate near the interface.

Figure 7 shows the through-thickness residual stress distribution for a tungsten carbide/cobalt (WC-Co) matrix coating. The coating was applied by a proprietary HVOF system designated herein as HVOF-A. The Ti-6Al-4V substrate was not

stress relieved. Specimens were grit blasted, and no preheat was applied prior to coating. Final coating thickness was approximately 0.254 mm (0.010 in.). A substrate modulus of 103.0 GPa (15.0×10^6 psi) and a Poisson's ratio of 0.3 were used for the analysis. Coating properties were assumed to be the same as those of the titanium substrate, as more precise values were not known. Because the coatings in this system were much thinner than the substrate, this assumption introduced very little error in the analysis.

Figure 8 shows the through-thickness residual stress distribution for another WC/Co matrix coating, designated in this paper as HVOF-B. The Ti-6Al-4V substrate was not stress relieved. No grit blasting or preheating was performed prior to coating. The final coating thickness was approximately 0.254 mm (0.010 in.). A substrate modulus of 103.0 GPa (15.0×10^6 psi) and a Poisson's ratio of 0.3 were used for the analysis. Coating properties were assumed to be the same as those of the titanium substrate, as precise values were not known.

Note that Fig. 7 shows a tensile stress through the thickness of the coating, whereas Fig. 8 shows a compressive stress. Since coatings applied by HVOF-A and HVOF-B are similar, it can be concluded that the application process and spray parameters can greatly influence the residual stress state. While only one residual stress specimen was used for each tungsten carbide coating, the reproducibility found for specimens represented in Fig. 1 to 6 provide confidence in the residual stresses obtained for these two tungsten carbide coatings.

Figure 9 shows the through-thickness residual stress distribution for a zirconia/8% yttria-stabilized thermal barrier coating

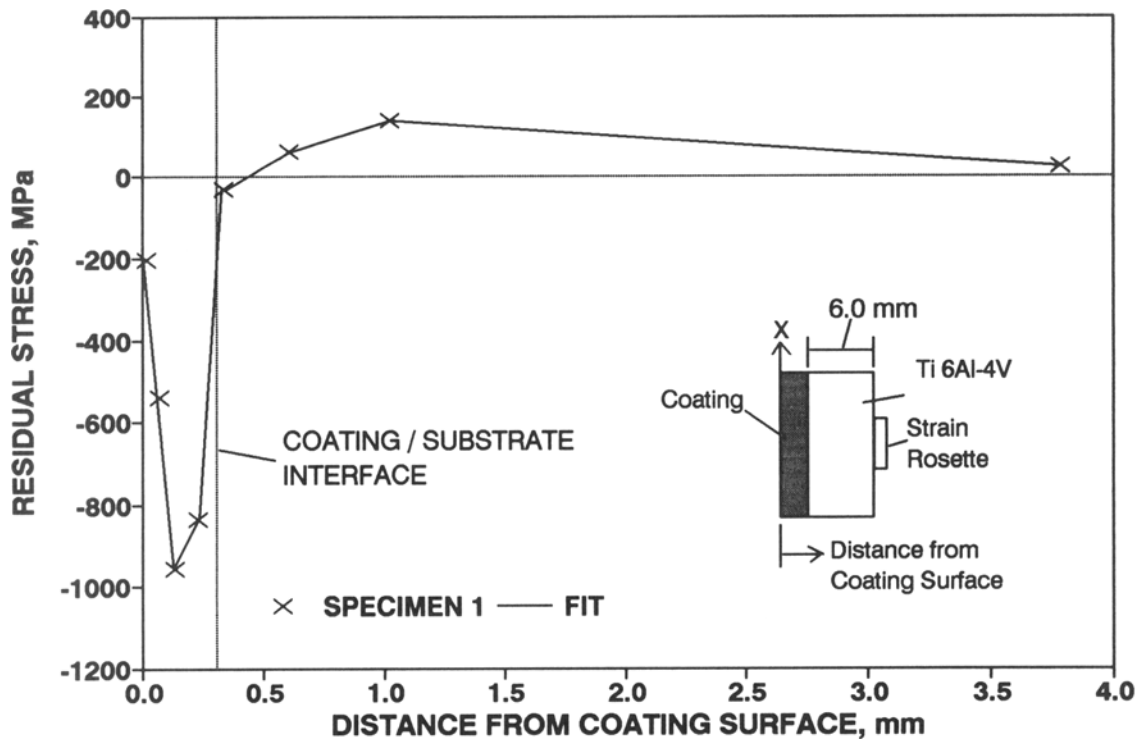


Fig. 8 Residual stress distribution for WC-Co coating applied by HVOF-B on a titanium substrate

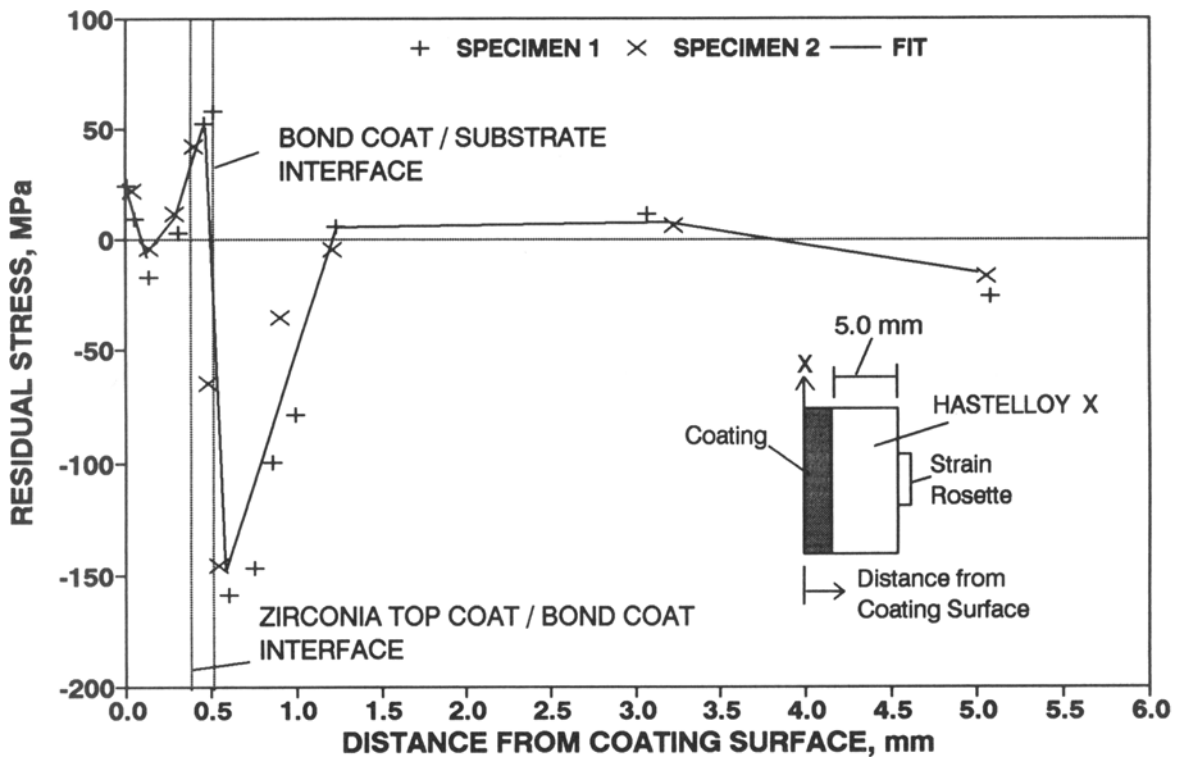


Fig. 9 Residual stress distribution for zirconia/8% yttria-stabilized thermal barrier coating with NiCoCrAlY bond coat

with a bond coating of NiCoCrAlY. A plasma spray process was used for application of the coatings. The substrate was Hastelloy Alloy X and was not stress relieved. No grit blasting or preheat-

ing was applied prior to coating. The coating thickness was approximately 0.254 mm (0.010 in.) with a bond coat thickness of approximately 0.076 mm (0.003 in.). A substrate modulus of

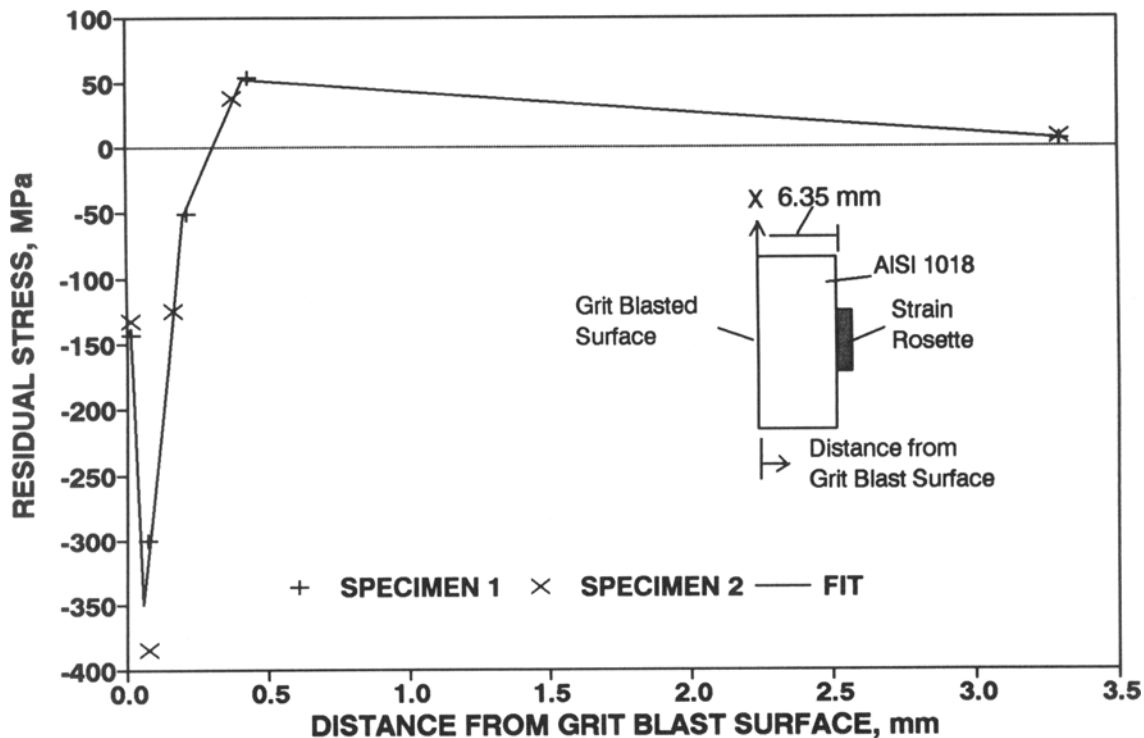


Fig. 10 Residual stress distribution for grit-blasted AISI 1018 specimens without coating

196.5 GPa (28.5×10^6 psi) and a Poisson's ratio of 0.3 were used for analysis. The coating properties are proprietary and are not reported here.

Interest in residual stress effects that may result from grit blasting the substrate has arisen due to the observed trend of high compressive stresses in the substrate just below the interface in many thermal spray coatings with tensile residual stresses. To help address the question as to the extent that grit blasting introduces compressive residual stress in the substrate prior to coating, residual stress evaluations were also conducted on grit-blasted, stress-relieved specimens of AISI 1018 steel without coating. Figure 10 shows the compressive stress in the substrate as a result of the grit-blasting process.

6. Conclusions

The through-thickness residual stress state of a thermal spray coating is an important characteristic in terms of coating integrity. Information about residual stresses in a coating is necessary to develop residual stress control strategies, to perform debonding analysis, and to predict service life. The modified layer-removal method for thermal spray coatings was developed and validated for evaluating residual stresses in coatings. The method was experimentally applied to several typical industrial thermal spray coatings. Results were found to be reproducible.

Results in Table 2 show that, for the cases considered, the modified layer-removal method is better suited for calculating residual stresses in thermal spray coatings than the conventional layer-removal method. Currently, accurate mechanical properties of thermal spray coatings are difficult to obtain. However, for the modified layer-removal method, strain-gage readings are

obtained from the substrate, which usually has known mechanical properties. Results in Table 3 show that, for the cases considered, a 20% uncertainty in the Young's modulus or Poisson's ratio of the coating leads to only very small errors in residual stresses computed using the modified layer-removal method. For other methods, such as x-ray diffraction or conventional hole drilling, a 20% uncertainty in Young's modulus corresponds to a 20% error in computed residual stress.

One goal of this paper was to demonstrate the application of the modified layer-removal method to a variety of industrial coatings. Residual stresses found in this work were in the range of -900 MPa (compressive) to 300 MPa (tensile). The highest tensile stresses were found for the WC-Co HVOF-A coating. The lowest tensile stresses were found for the zirconia thermal-barrier coating. An interesting result was the compressive residual stresses found for the WC-Co HVOF-B coating.

Acknowledgments

The authors acknowledge Robert Unger and Peter Kutsopias of Hobart Tafa Inc. (Concord, New Hampshire) for providing the equipment and materials for the Ni-5Al coatings, Willard Emery and David Somerville of Southwest Aeroservice (Tulsa, Oklahoma) for providing the spraying services for the Ni-5Al coatings, and Jan Wigren and Göran Sjöberg of Volvo Aero Corporation (Trollhättan, Sweden) for providing tungsten carbide and thermal-barrier coated specimens evaluated in this study.

References

1. K.G. Budinski, *Surface Engineering for Wear Resistance*, Prentice Hall, 1988

2. M.K. Hobbs and H. Reiter, Residual Stresses in ZrO₂-8%Y₂O₃ Plasma Sprayed Thermal Barrier Coatings, *Thermal Spray: Advances in Coatings Technology*, D.L. Houck, Ed., ASM International, 1988, p 285-290
3. E.F. Rybicki and R.B. Stonesifer, An LEFM Analysis for the Effects of Weld Repair Induced Residual Stresses on the Fracture of HSST ITV-8, *J. Pressure Vessel Technol.*, Vol 102, Aug 1980, p 318-323
4. M. Gudge, D.S. Rickerby, K.T. Kingswell, and T. Scott, Residual Stress in Plasma Metallic and Ceramic Coatings, *Thermal Spray Research and Applications*, T.F. Bernecki, Ed., ASM International, 1991, p 331-337
5. T. Morishita, R.W. Whitfield, E. Kuramochi, and S. Tanabe, Coatings with Compressive Stress, *Thermal Spray: International Advances in Coatings Technology*, C.C. Berndt, Ed., ASM International, 1992, p 1001-1004
6. M.E. Woods, Thermal Fatigue Rig Testing of Thermal Barrier Coatings for Internal Combustion Engines, *Thermal Spray Technology—New Ideas and Processes*, D.L. Houck, Ed., ASM International, 1989, p 245-253
7. F. Bordeaux, R.G. Saint-Jacques, C. Moreau, S. Dallaire, and J. Lu, Thermal Shock Resistance of TiC Coatings Plasma-Sprayed on Macroroughened Substrates, *Thermal Spray Coatings: Properties, Processes and Applications*, T.F. Bernecki, Ed., ASM International, 1992, p 127-134
8. T. Konaga, H. Kohno, and H. Manabe, X-ray Diffraction Technique for Measuring Stress in Coatings, *Residual Stresses Sci. Technol.*, Vol 1, 1987, p 191-222
9. "Measurement of Residual Stresses by the Hole-Drilling Strain Gage Method," Tech. Note TN-503-3, Measurements Group, Raleigh, NC, 1988
10. D.J. Greiving, J.R. Shadley, and E.F. Rybicki, Effects of Coating Thickness and Residual Stresses on the Bond Strength of ASTM C633-79 Thermal Spray Coating Test Specimens, *1994 Thermal Spray Industrial Applications*, C.C. Berndt and S. Sampath, Ed., ASM International, 1994, p 639-645
11. SAE J936, "Methods of Residual Stress Measurement," *Handbook Supplement J936*, Society of Automotive Engineers, Dec 1965
12. Y.C. Kim, T. Terasaki, and T.H. North, A Method of Measuring the Through-Thickness Residual Stress in a Thermally-Sprayed Coating, *Thermal Spray Coatings: Properties, Processes and Applications*, T.F. Bernecki, Ed., ASM International, 1992, p 221-227
13. R.M. Jones, *Mechanics of Composite Materials*, Hemisphere Publishing, 1975
14. J.R. Shadley, E.F. Rybicki, and W.S. Shealy, Application Guidelines for the Parting-Out Step in a Through-Thickness Residual Stress Measurement Procedure, *Strain*, Nov 1987, p 157-166
15. Stress-Relief Heat Treating of Steel, *ASM Handbook*, Vol 4, *Heat Treating*, ASM International, 1991, p 33-34